[16] K. Gosalia, M. Humayun, and G. Lazzi, "Impedance matching and implementation of planar space-filling dipoles as intraocular implanted antennas in a retinal prosthesis," *IEEE Trans. Antennas Propag.*, vol. 53, no. 8, pp. 2365–2373, Aug. 2005.
[17] E. Chow, C.-L. Yang, A. Chlebowski, S. Moon, W. Chappell, and P. Irazoqui, "Implantable wireless telemetry boards for *in vivo* transocular transmission," *IEEE Trans. Microw. Theory Tech.*, vol. 56, no. 12, pp. 3200–3208, Dec. 2008.
[18] P. Soontornpipit, C. Furse, and Y. C. Chung, "Design of implantable microstrip antenna for communication with medical implants," *IEEE Trans. Microw. Theory Tech*, vol. 52, no. 8, pp. 1944–1951, Aug. 2004.
[19] S. Soora, K. Gosalia, M. Humayun, and G. Lazzi, "A comparison of two and three dimensional dipole antennas for an implantable retinal prosthesis," *IEEE Trans. Antennas Propag.*, vol. 56, no. 3, pp. 622–629, Mar. 2008.
[20] K. Takahata, Y. Gianchandani, and K. Wise, "Micromachined antenna stents and cuffs for monitoring intraluminal pressure and flow," *J. Microelectromech. Syst.*, vol. 15, no. 5, pp. 1289–1298, Oct. 2006.
[21] E. Chow, Y. Ouyang, B. Beier, W. Chappell, and P. Irazoqui, "Evaluation of cardiovascular stents as antennas for implantable wireless applications," *IEEE Trans. Microw. Theory Tech.*, vol. 57, no. 10, pp. 2523–2532, Oct. 2009.
[22] H. A. Wheeler, "Fundamental limitations of a small VLF antenna for submarines," *IRE Trans. Antennas Propag.*, vol. 6, no. 1, pp. 123–125, 1958.
[23] R. F. Fano, L. J. Chu, and R. B. Adler, *Electromagnetic Fields, Forces and Energy*, 1st ed. New York: Wiley, 1960, ch. 6.
[24] H. A. Wheeler, "Fundamental limitations of small antennas," *Proc. I.R.E.*, vol. 35, no. 12, pp. 1479–1484, Dec. 1947.
[25] H. A. Wheeler, *Small Antennas*, vol. 23, no. 4, pp. 462–469, Jul. 1975.
[26] H. A. Wheeler, "A helical antenna for circular polarization," *Proc. I.R.E.*, vol. 35, no. 12, pp. 1484–1488, Dec. 1947.
[27] J. D. Kraus, "The helical antenna," *Proc. I.R.E.*, vol. 37, no. 3, pp. 263–272, Mar. 1949.
[28] J. D. Kraus and R. J. Marhefka, *Antennas for All Applicaions*, 3rd ed. New York: McGraw Hill, 2002, ch. 8.
[29] Dielectric Properties of Tissues [Online]. Available: http://niremf.ifac.cnr.it/tissprop/
[30] P. Nikitin, K. Rao, and S. Lazar, "An overview of near field UHF RFID," in *Proc. IEEE Int. Conf. on RFID*, Mar. 2007, pp. 167–174.
[31] *IEEE Recommended Practice for Measurements and Computations of Radio Frequency Electromagnetic Fields With Respect to Human Exposure to Such Fields, 100 kHz to 300 GHz*, EEE Std C95.3-2002 (R2008), Jun. 2008.
[32] P. Riu and K. Foster, "Heating of tissue by near-field exposure to a dipole: A model analysis," *IEEE Trans. Biomed. Eng.*, vol. 46, no. 8, pp. 911–917, Aug. 1999.
[33] L. Xu, M.-H. Meng, H. Ren, and Y. Chan, "Radiation characteristics of ingestible wireless devices in human intestine following radio frequency exposure at 430, 800, 1200, and 2400 MHz," *IEEE Trans. Antennas Propag.*, vol. 57, no. 8, pp. 2418–2428, Aug. 2009.
[34] Environmental Health Criteria 137 (1993): Electromagnetic Fields (300 Hz–300 GHz) WHO, Geneva, Switzerland, 1993 [Online]. Available: http://www.inchem.org/documents/ehc/ehc/ehc137.htm
[35] K. Yekeh and R. Kohno, "Wireless communications for body implanted medical device," in *Proc. Asia-Pacific Microwave Conf. Asia-Pacific*, Dec. 2007, pp. 1–4.
[36] R. W. P. King and G. S. Smith, *Antennas in Matter—Fundamentals, Theory and Applications*, 1st ed. Cambridge, MA: MIT Press, 1981, ch. 8.
[37] *Bioengineering and Biophysical Aspects of Electromagnetic Fields*, F. S. Barnes and B. Greenebaum, Eds., 3rd ed. Baca Raton, FL: CRC Press, 2007, ch. 3.
[38] "Guidelines for Limiting Exposure to Time-Varying Electric, Magnetic, and Electromagnetic Fields (up to 300 GHz)," International Committee for Non-ionizing Radiation Protection (ICNIRP), 1998 [Online]. Available: http://www.icnirp.de/documents/emfgdl.pdf
[39] *IEEE Standard for Safety Levels with Respect to Human Exposure to Radio Frequency Electromagnetic Fields, 3 kHz to 300 GHz*, IEEE Std C95.1-2005, Apr. 2006.
[40] A. J. Johansson, "Performance measures of implant antennas," in *Proc. 1st Eur. Conf. on Antennas Propag.*, Nov. 2006, pp. 1–4.
[41] L. Chirwa, P. Hammond, S. Roy, and D. Cumming, "Electromagnetic radiation from ingested sources in the human intestine between 150 MHz and 1.2 GHz," *IEEE Trans. Biomed. Eng.*, vol. 50, no. 4, pp. 484–492, Apr. 2003.
[42] S. I. Kwak, K. Chang, and Y. J. Yoon, "The helical antenna for the capsule endoscope," in *Proc. IEEE Antennas and Propagation Society Int. Symp.*, Jul. 2005, vol. 2B, pp. 804–807.
[43] *Electromagnetic Compatibility and Radio Spectrum Matters (ERM); Short Range Devices (SRD); Radio equipment to be Used in the 25 MHz to 1000 MHz Frequency Range With Power Levels Ranging up to 500 mW; Part 1: Technical Characteristics and Test Methods*, ESTI Standard, EN 300 220-1 V2.3.1, 2010.
[44] CST, Computer Simulation Software [Online]. Available: http://www.cst.com/Content/Applications/Markets/MWandRF.aspx
[45] K. Ito, K. Furuya, Y. Okano, and L. Hamada, "Development and characteristics of a biological tissue-equivalent phantom for microwaves," *Electron. Commun. Jpn. (Part I: Commun.)*, vol. 84, no. 4, pp. 67–77, Dec. 2000.

A Novel Folded UWB Antenna for Wireless Body Area Network

Cheng-Hung Kang, Sung-Jung Wu, and Jenn-Hwan Tarng

***Abstract*—A novel folded ultrawideband antenna for Wireless Body Area Network (WBAN) is proposed, which can effectively reduce the backward radiation and proximity effects of human bodies. The proposed antenna has a low-profile 3D structure that consists of a bevel-edge feed structure and a metal plate with folded strip. The bevel edge feed structure achieves broadband impedance matching and the metal plate acts as the main radiator. Moreover, the folded strip not only extends the lower frequency band but also provides additional resonant frequency around 6 GHz. The final bandwidth covers from 3.1 GHz to 12 GHz. The proposed antenna shows the directional patterns with low backward radiation due to the patch-like structure and the ground plane also prevents from the proximity effects of human bodies. Furthermore, the simulated SAR values of the proposed antenna are lower than the values of omnidirectional disc planar monopole. These features demonstrate that the proposed antenna is suitable for WBAN application.**

***Index Terms*—Body-area network, 3-D antenna, ultrawideband.**

I. Introduction

Wireless body area network (WBAN), a communication system which transmits large amount of information/data near the human body, is attracting more and more attention in wireless communications [1]. WBAN integrated with proper sensors can observe and transmit vital signs of patients, police or fire personnel without cables. With increasing attention directed toward WBAN, the ultrawideband (UWB) technology becomes an active solution for these applications because of its low transmission power and high data rates.

The antenna and propagation measurements for WBAN are discussed in [2], [3]. The results show that the path loss and the rms delay spread are highly related to antenna structure. Several studies provide various antenna designs used in WBAN [4]–[7]. In [2], a 3-D monopole antenna placed perpendicular to the human body is designed for WBAN. However, the 3-D monopole antenna is too high so it

Manuscript received May 21, 2010; revised May 15, 2011; accepted July 25, 2011. Date of publication October 24, 2011; date of current version February 03, 2012. This work was supported by the National Science Council, R.O.C., under Grants NSC-99-2219-E-009-001 and NSC-99-2221-E-009-028-MY2.

The authors are with National Chiao Tung University, Hsinchu, Taiwan 300, ROC (e-mail: chkang.cm97g@g2.nctu.edu.tw).

Color versions of one or more of the figures in this comunication are available online at http://ieeexplore.ieee.org.

Digital Object Identifier 10.1109/TAP.2011.2173101

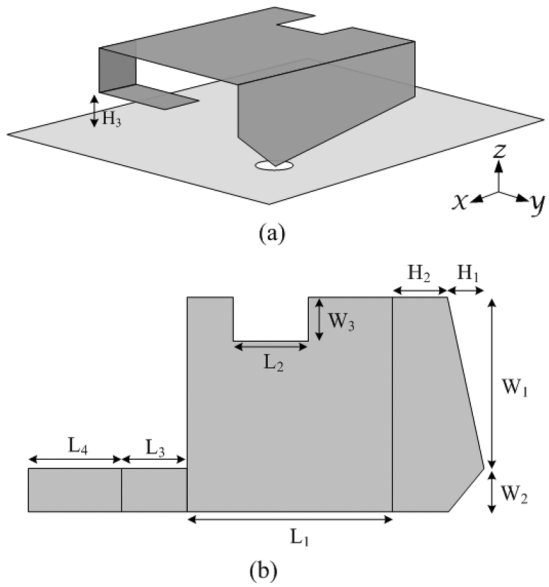

Fig. 1. (a) Configuration of the proposed ultrawideband antenna. (b) The antenna unbent into a planar structure.

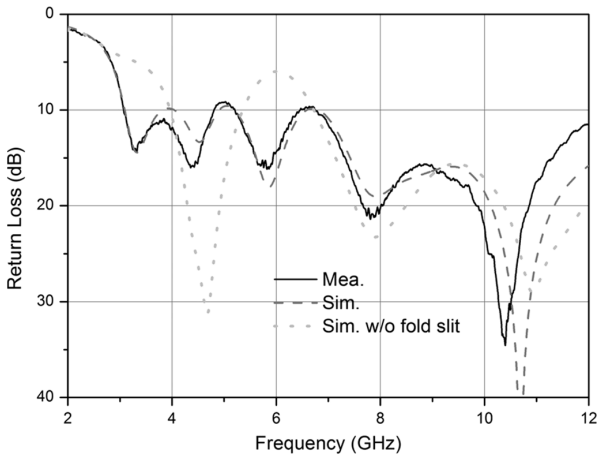

Fig. 2. Measured and simulated return loss of the proposed antenna.

will obstruct the human daily activities when applied to the human body. Therefore, planar monopole antennas with low antenna height are widely developed in the UWB community. However, when these antennas lie on the human body, the operating frequency, bandwidth and radiation efficiency are easily interfered with by the human body. Except the aforementioned influences, specific absorption rate (SAR) is another important issue in WBAN. In [5], it has been shown simulated results that the antenna with omnidirectional pattern exhibits low radiation efficiency and high SAR values compared to directional antenna when placed on human model.

Low backward radiation, low height with compact form, and low mutual effect between the antenna and the human body are three major requirements [5]–[7] for WBAN antennas. These features increase the difficulty of antenna design. To solve this issue, some studies propose using a reflector in antenna design to reduce the backward radiation and enhance directionality. In [5], a reflector was added to a 3 GHz–6 GHz slot antenna and this additional reflector enhanced the directionality and radiation efficiency. But the additional reflector affects the antenna bandwidth which becomes 4 GHz to 6.5 GHz and is not wide enough for the UWB system.

In this communication, a novel directional UWB antenna is proposed for the WBAN application. The proposed antenna consists of a bevel

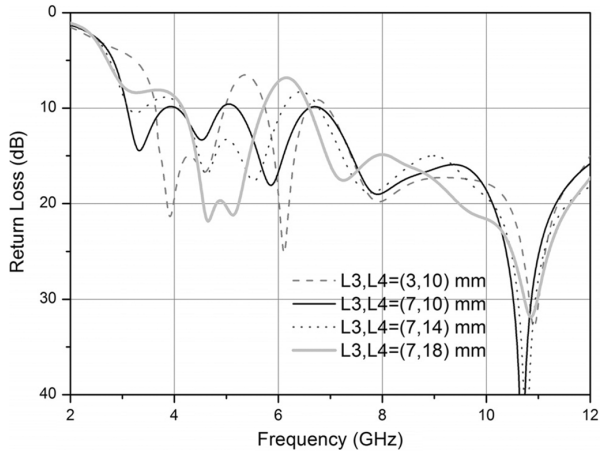

Fig. 3. Simulated return loss of various lengths of L_3 and L_4.

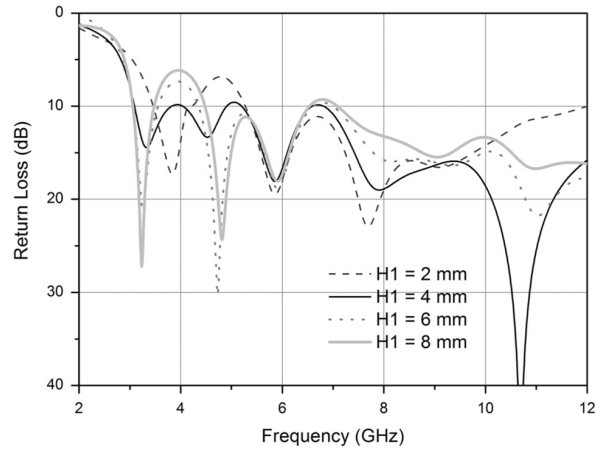

Fig. 4. Simulated return loss of various lengths of H_1.

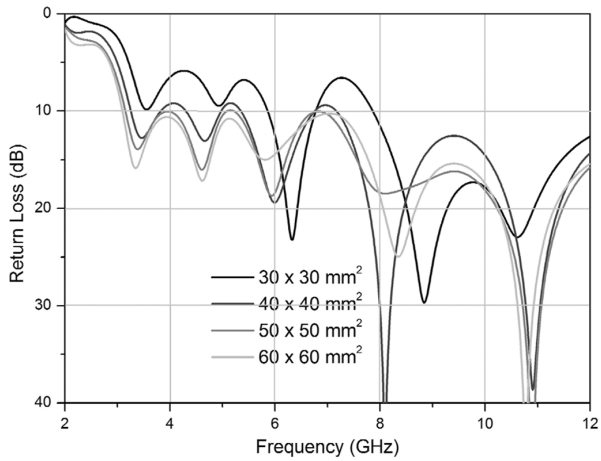

Fig. 5. Simulated return loss of various ground size.

edge feed structure and a truncated metal plate with folded strip. The size of the proposed antenna is $25 \times 22 \times 10$ mm^3 with ground plane 50×50 mm^2 and the bandwidth covers from 3.1 GHz to 12 GHz. Section II presents the geometry and design concept of the proposed antenna. The design parameters and simulated SAR values are also introduced in Section II. Radiation patterns are shown in Section III. Finally, Section IV draws some conclusions.

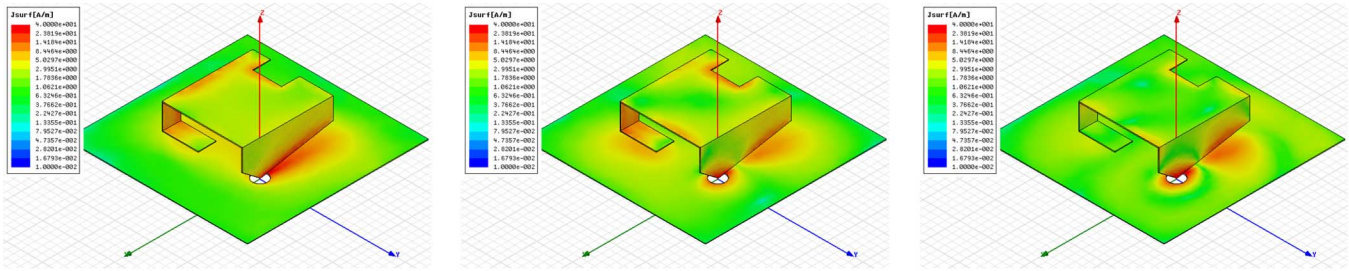

Fig. 6. Current distribution of the proposed antenna at (a) 4 GHz, (b) 7 GHz, (c) 10 GHz.

II. Antenna Design Concept and Performance

Fig. 1 shows the geometry of the proposed antenna. The proposed antenna consists of a bevel edge feed structure and a truncated metal plate with folded strip. To enlarge bandwidth, the bevel edge structure achieves slow impedance variation by using traveling wave concept. The metal plate is designed as a main radiator. The truncated edge and the folded strip of the metal plate extend the current path to lower the operating frequency. In addition, because of the patch-like structure, the wave radiates toward the z direction and the ground plane reduces the backward radiation. The whole antenna size is 25 mm × 22 mm × 10 mm with a 50 mm × 50 mm ground plane. The final parameters of the proposed antenna are $H_1 = 4$ mm, $H_2 = 6$ mm, $H_3 = 3$ mm, $W_1 = 20$ mm, $W_2 = W_3 = 5$ mm, $L_1 = 22$ mm, $L_2 = 8$ mm, $L_3 = 7$ mm, $L_4 = 10$ mm.

Fig. 2 shows the simulated and measured return losses. The simulation was performed using a commercial simulator while the measurements were taken by an E8364B network analyzer. The measured bandwidth covers from 3.1 GHz to 12 GHz and agrees with the simulated results. The minor discrepancies of simulation and measurement may be attributed to the connector, which is not considered in the simulation. Fig. 2 also shows the simulated result of the proposed antenna without the folded strip. It is evidenced that the folded strip not only determines the lower operating frequency from 3 to 4 GHz but also creates an additional resonant frequency around 6 GHz. The folded strip is the key factor of antenna design.

The effect of folded strip is presented in Fig. 3. The folded strip extends the current path and creates lower resonant frequencies. According to Fig. 3, the length of L_3 affects the lowest frequency and when the length of L_4 increases, the impedance in the middle frequency becomes mismatched. By suitably adjusting the length of the strip, we can make the whole frequency band under the 10 dB return loss condition.

The effect of the feed structure is shown in Fig. 4. The tapered profile of the feed structure achieves the slow impedance variation for obtaining the ultra-wide bandwidth. The slope of the bevel edge should be carefully designed to achieve wideband matching. In our experiments, the H_1 should be 4 mm to obtain better impedance matching for the whole operating frequency.

Fig. 5 shows the parametric simulations with regard to the different ground plane size. For the proposed antenna which radiates as a patch antenna, the ground plane should be large enough to resonant the desired frequency. In the simulating results, it can be observed that the impedance match is interfered and the bandwidth becomes narrow when the ground plane becomes 30×30 mm^2 which is close to the main radiator. Therefore, the ground plane size of the proposed antenna should be larger than 40×40 mm^2 to generate the wanted resonance mode. In the final design, 50×50 mm is chosen for the ground plane by the dimension and better impedance match.

Furthermore, the current distribution of the proposed antenna in 4 GHz, 7 GHz and 10 GHz is exhibited in Fig. 6. In the low frequency, the current distributes along the edge of the truncated plate and the folded strip, which is like a patch antenna. Therefore, the truncated part and the length of the folded strip determines the lowest frequency. In addition, a resonance mode can be observed at the folded strip in middle band. For high band, the tapered profile fed structure travels the energy to the plate and radiate as combination of general monopole and patch antenna. Moreover, the shape of the tapered profile crucially affects the impedance match within the whole band. The proposed antenna combines the patch-like radiator and traveling wave concept to achieve the ultra-wide bandwidth and directional patterns.

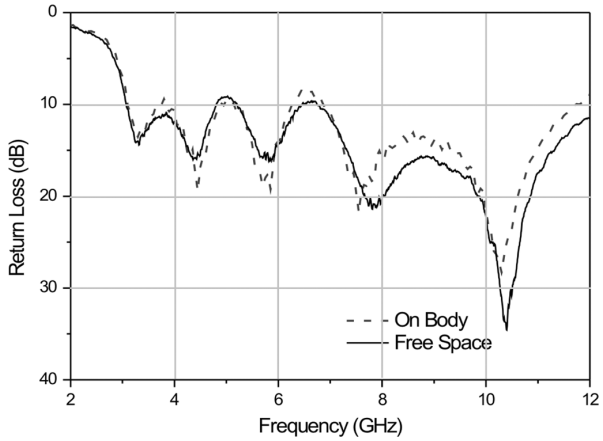

Fig. 7. Comparison measured return loss between in free space and on the body.

In order to verify the proximity effect of human body, return loss of the proposed antenna in free space and on the body are measured, as shown in Fig. 7. The spacing between the proposed antenna and the human skin is 2 mm. The proximity effect of the human body slightly affects the impedance matching of the proposed antenna because that directivity of the proposed antenna is outward from the human body.

Furthermore, a truncated body model is considered in simulation to estimate the specific absorption rate (SAR) value and radiation efficiency by software SEMCAD X. Two different body model is considered in the simulations, one is single layer muscle model and another is three layers body model with skin, fat and muscle according to the [5]. Full dimensions of the models are skin: $120 \times 110 \times 1$ mm^3 with $\varepsilon_r = 38$, $\sigma = 2.7$ [S/m], fat: $120 \times 110 \times 3$ mm^3 with $\varepsilon_r = 5.1$, $\sigma = 0.18$ [S/m] and muscle: $120 \times 110 \times 40$ mm^3 with $\varepsilon_r = 50.8$, $\sigma = 3$ [S/m] according to [5]. Moreover, in order to reveal the SAR values in relative way, a planar disc monopole antenna with omnidirection pattern, as shown in Fig. 8, is also involved in the simulation for comparison. For keeping the same distance from the model to the top of the antenna (antenna height: 10 mm), the proposed antenna is 1 mm away from the body model and the planar disc monopole antenna (antenna height: 1.6 mm) is 10 mm away from the body model. Table I shows the simulated results of peak SAR values and the total radiation efficiency included the muscle and body models. As expected, the SAR values of the proposed antenna are lower than one of the planar UWB monopole antenna due to the patch-like structure and directional patterns of the proposed antenna.

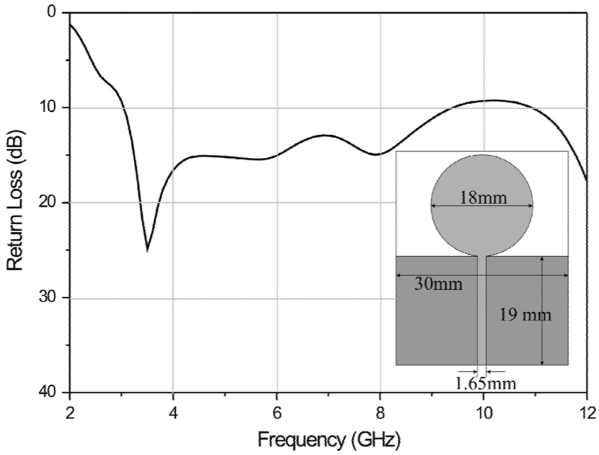

Fig. 8. Geometry of the planar disc monopole antenna and its simulated return loss.

TABLE I
PEAK SAR VALUES AND RADIATION EFFICIENCY (NORMALIZE TO 1 W)

Frequency	4 GHz		7 GHz	
	Radiation effiency (%)	SAR 10g (W/kg)	Radiation effiency (%)	SAR 10g (W/kg)
The proposed antenna–1 layer model	88.24%	0.699	79.32%	1.38
The proposed antenna-3 layers model	84.33%	1.073	84.2%	2.11
The disc planar monopole antenna-1 layer model	64.38%	7.486	79.35%	4.85
The disc planar monopole antenna-3 layers model	40.64%	11.195	80.17%	4.99

(Pin=1W)

III. RADIATION PATTERNS

The antenna power gain radiation patterns in free space are measured in an anechoic chamber with an Agilent E362B network analyzer and NSI2000 far-field measurement software. The xz- and yz-plane radiations at 4 GHz, 7 GHz and 10 GHz are illustrated in Fig. 9. The measured patterns agree with the simulated patterns while some minor discrepancies of simulation and measurement in xy-plane and yz-plane can be attributed to the interference of the coaxial cable and the absorber. The radiations perform directional patterns in xz-plane with peak gains of 5.8 dBi, 4 dBi, and 3 dBi for each frequency, respectively. In the yz-plane, the radiation patterns on the whole operating frequency are nearly directional patterns. The power levels of backward radiation are less than -5 dBi. It is evidenced that the proposed antenna is desirable in WBANs applications to reduce the backward radiation.

IV. CONCLUSION

A novel folded UWB antenna for WBAN applications has been proposed. The proposed antenna utilizes the bevel edge feed structure and the truncated metal plate with folded strip to achieve ultrawide bandwidth from 3.1 GHz to 12 GHz. The effects of the feed structure and the truncated metal plane are discussed in order to provide brief guidelines. The measured results show that the antenna is only slightly affected by the proximity effect of human body. Moreover, the simulated SAR values are lower than the omnidirectional disc planar monopole. The patch-like structure can reduce the backward radiation and enhance the directionality. These features demonstrate that the proposed antenna is suitable for WBAN applications.

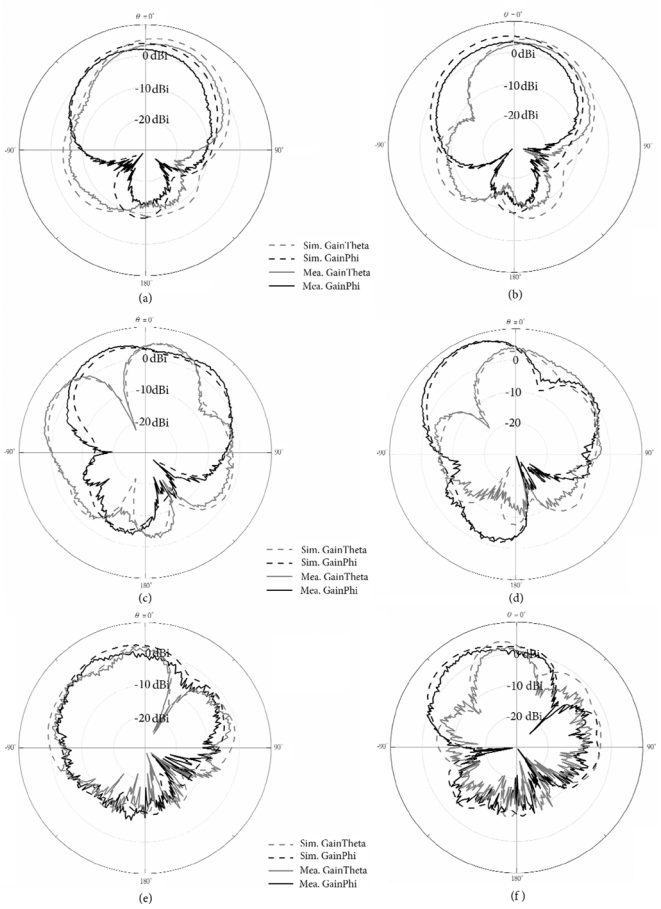

Fig. 9. Simulated and measured radiation patterns (a) at 4 GHz XZplane, (b) at 4 GHz YZplane, (c) at 7 GHz XZplane, (d) at 7 GHz YZplane, (e) at 10 GHz XZplane, (f) at 10 GHz YZplane.

REFERENCES

[1] T. Zasowski, F. Althaus, M. Stager, A. Wittneben, and G. Troster, "UWB for noninvasive wireless body area networks: Channel measurements and results," in *Proc. IEEE Conf. Ultra Wideband Systems and Technologies*, Reston, VA, Nov. 2003, pp. 285–289.

[2] A. Alomainy, Y. Hao, C. G. Parini, and P. S. Hall, "Comparison between two different antennas for UWB on-body propagation measurements," *IEEE Antennas Wireless Propag. Lett.*, vol. 4, pp. 31–34.

[3] A. Alomainy, A. Sani, A. Rahman, J. G. Santas, and H. Yang, "Transient characteristics of wearable antennas and radio propagation channels for ultrawideband body-centric wireless communications," *IEEE Trans. Antennas Propag.*, vol. 57, no. 4, pp. 875–884, 2009.

[4] M. Klemm and G. Troester, "Textile UWB antennas for wireless body area networks," *IEEE Trans. Antennas Propag.*, vol. 54, no. 11, pp. 3192–3197, 2006.

[5] M. Klemm, I. Z. Kovcs, G. F. Pedersen, and G. Troster, "Novel small-size directional antenna for UWB WBAN/WPAN applications," *IEEE Trans. Antennas Propag.*, vol. 53, no. 12, pp. 3884–3896, 2005.

[6] Z. Shaozhen and R. Langley, "Dual-band wearable textile antenna on an EBG substrate," *IEEE Trans. Antennas Propag.*, vol. 57, no. 4, pp. 926–935, 2009.

[7] N. Haga, K. Saito, M. Takahashi, and K. Ito, "Characteristics of cavity slot antenna for body-area networks," *IEEE Trans. Antennas Propag.*, vol. 57, no. 4, pp. 837–843, 2009.

[8] G. A. Conway and W. G. Scanlon, "Antennas for over-body-surface communication at 2.45 GHz," *IEEE Trans. Antennas Propag.*, vol. 57, no. 4, pp. 844–855, 2009.